❏   1

Improvements the direct torque control performance for an induction machine using fuzzy logic controller

Radouan Gouaamar[1], Seddik Bri[1], Zineb Mekrini[2]
[1]Materials and Instrumentation, Electrical Engineering, High School of Technology, Moulay Ismail University, Meknes, Morocco
[2]Industrial Systems Engineering and Energy Conversion Team, Faculty of Sciences and Technology of Tangier,
Abdelmalek Essaadi University, Tetouan, Morocco

Article Info	ABSTRACT
	This article examines a solution to the major problems of induction machine control in order to achieve superior dynamic performance. Conventional direct torque control and indirect control with flux orientation have some drawbacks, such as current harmonics, torque ripples, flux ripples, and rise time. In this article, we propose a comparative analysis between previous approaches and the one using fuzzy logic. Results from the simulation show that the direct torque control method using fuzzy logic is more effective in providing a precise and fast response without overshooting, and it eliminates torque and flux fluctuations at low switching frequencies. The demonstrated improvements in dynamic performance contribute to increased operational efficiency and reliability in industrial applications.

Corresponding Author:

Radouan Gouaamar
Materials and Instrumentation, Electrical Engineering, High School of Technology, Moulay Ismail University
Meknes, Morocco
Email: radouan.gouaamar@gmail.com

1. INTRODUCTION

Electric motors are essential components in the industrial sector, with three-phase asynchronous motors being particularly significant. They account for approximately 80% of industrial control systems [1], [2]. These motors are highly valued for their reliability, straightforward design, cost-effectiveness, and minimal maintenance requirements. However, their modeling presents challenges due to their dynamic and nonlinear nature, complex equations, and difficult-to-measure state variables [3], [4]. Consequently, advanced control algorithms are necessary to ensure effective real-time control of torque and flux [5], [6]. One prominent control technique developed in the 1970s is field-oriented control (FOC), which offers the advantage of decoupling electromagnetic torque and flux. This enables a prompt torque response, a broad range of speed regulation, and high efficiency across a variety of loads [7], [8]. Nevertheless, field-oriented control (FOC) can be intricate and susceptible to motor parameter variations [9]. To address these challenges, a novel approach known as direct torque control (DTC) was first introduced by Takahashi and Noguchi in the early 1980s [10]. DTC has attracted considerable attention due to its advantageous features, including a straightforward structure, dynamic response, and reduced reliance on machine parameters. Importantly, DTC eliminates the necessity for current regulation and coordinate transformations [11], [12].

However, there are two significant drawbacks to this approach: uncontrolled flux and torque ripples, as well as variable switching frequency [13], [14]. These ripples create additional noise and vibrations, which can result in fatigue and wear of the machine shaft. In order to mitigate these effects, the integration of intelligent techniques is seen as advantageous [15], [16].

This article focuses on investigating the potential of utilizing fuzzy logic-based DTC to enhance the performance of current control methods. Our research suggests using a fuzzy logic controller in place of the switching selection block and the two hysteresis controllers. By implementing this fuzzy logic controller, the output parameters of the asynchronous machine can be effectively regulated to their desired reference values within a predetermined timeframe. The primary objectives of our study revolve around achieving the following goals: minimizing response time, reducing flux and torque oscillations, and reducing the stator current's overall harmonic distortion (THD).

This article is organized manner: section 2 provides a detailed introduction to the modeling of the asynchronous motor, offering a comprehensive overview of its characteristics. In section 3, the control method is extensively discussed, emphasizing its fundamental principles and key features. To verify and assess the performance of the suggested strategy, section 4 presents the simulation results obtained using the MATLAB/Simulink environment. This section allows for a meticulous examination and comparison of the outcomes. The article concludes in section 5 with a summary of the key conclusions drawn from the research and helpful suggestions for future research directions.

2. INDUCTION MOTOR MODEL

It is generally acknowledged that the (α, β) reference frame, which symbolizes a two-phase model, is the best option for analyzing the dynamic behavior and developing control schemes for three-phase induction devices. This strategy makes the Triple-phase representation of the machine less complicated. The following are possible expressions for the electromagnetic equations that control induction motors [17]:

$$\frac{d}{dt}\begin{bmatrix} i_{s\alpha} \\ i_{s\beta} \\ \psi_{s\alpha} \\ \psi_{s\beta} \end{bmatrix} = \begin{bmatrix} -\frac{1}{\alpha}(\frac{1}{\tau_s}+\frac{1}{\tau_r}) & -w_r & \frac{1}{\alpha L_s \tau_r} & \frac{w_r}{\alpha L_s} \\ w_r & -\frac{1}{\alpha}(\frac{1}{\tau_s}+\frac{1}{\tau_r}) & -\frac{w_r}{\alpha L_s} & \frac{1}{\alpha L_s \tau_r} \\ -R_s & 0 & 0 & 0 \\ 0 & -R_s & 0 & 0 \end{bmatrix} \cdot \begin{bmatrix} i_{s\alpha} \\ i_{s\beta} \\ \psi_{s\alpha} \\ \psi_{s\beta} \end{bmatrix} + \begin{bmatrix} \frac{1}{\alpha L_s} & 0 \\ 0 & \frac{1}{\alpha L_s} \\ 1 & 0 \\ 0 & 1 \end{bmatrix} \cdot \begin{bmatrix} v_{s\alpha} \\ v_{s\beta} \end{bmatrix} \qquad (1)$$

In the equations provided, the following variables and parameters are defined: M is mutual inductance, w_r is rotor mechanical angular velocity, L_s is stator inductance, L_r is rotor inductance, R_s is stator resistance, Ω is mechanical speed, $i_{s\alpha,\beta}$ is currents of the stator, $v_{s\alpha,\beta}$ is stator voltage, $\psi_{s\alpha,\beta}$ is stator flux, J is inertia moment, and P is number of pole pairs. The parameters α, τ_r, and τ_s are defined as positive constants:

$$\tau_r = \frac{L_r}{R_r} \; ; \alpha = 1 - \frac{M^2}{L_s L_r} \; ; \tau_s = \frac{L_s}{R_s} \qquad (2)$$

The expressions for the electromagnetic torque and motion equations are as in (3), (4).

$$T_{em} = \frac{3}{2}p(\psi_{s\alpha}i_{s\beta} - \psi_{s\beta}i_{s\alpha}) \qquad (3)$$

$$J.\frac{d\Omega}{dt} + f.\Omega = T_{em} - T_r \qquad (4)$$

3. CONTROL METHOD
3.1. Direct torque control

Middle of the 1980s, Takahashi and Depenbrock first suggested the idea of direct torque control (DTC) as a control strategy for induction machines (IM). DTC offers several advantages over vector control, including reduced sensitivity to changes in machine parameters. It also features a simpler control algorithm that does away with the requirement for pulse width modulation (PWM), current controllers, or Park transforms. Moreover, DTC eliminates proportional-integral (PI) control loops, thereby enhancing dynamic performance and mitigating issues caused by proportional-integral regulator saturation. This enables DTC to achieve fast and accurate torque response, facilitating high-efficiency operation [18], [19].

The electromagnetic torque (T_{em}) and flux (ψ_s) of a machine can be controlled using the DTC method. The voltage inverter switches connected to the machine are directly controlled through a control sequence. To enable decoupled control and regulation of the machine's torque and flux, DTC makes use of two hysteresis regulators, a switching table, and other parts. Figure 1 illustrates the structural layout of the DTC control system. A three-level hysteresis controls the magnetic torque, while a two-level hysteresis regulates the flux. To create the best switching table, these comparators' outputs are combined with knowledge of the flux vector.
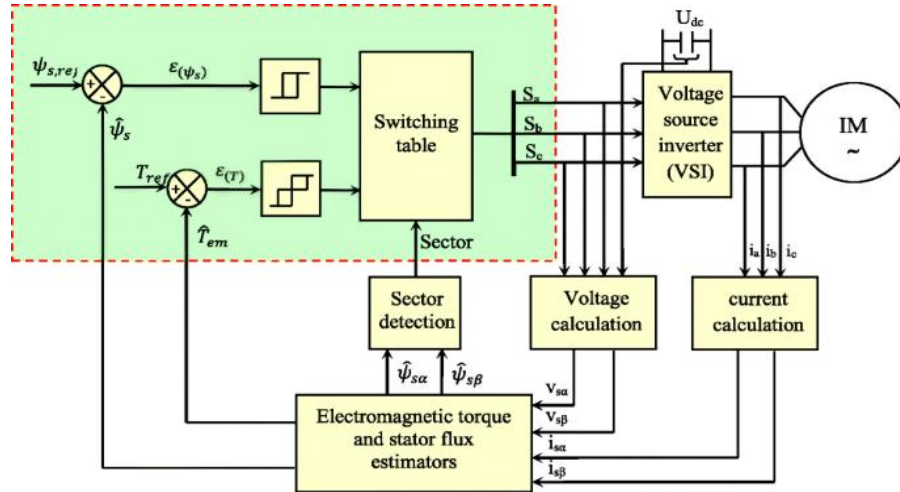
Figure 1. Diagram illustrating DTC for an induction motor

The estimations of T_{em} and the ψ_s are computed using (5) and (6).

$$\psi_s = \sqrt{\psi_{s\alpha}^2 + \psi_{s\beta}^2} \tag{5}$$

$$T_{em} = p(\psi_{s\alpha} i_{s\beta} - \psi_{s\beta} i_{s\alpha}) \tag{6}$$

The angle θ_s is derived through calculation from (7).

$$\theta_s = arctg\left(\frac{\psi_{s\alpha}}{\psi_{s\beta}}\right) \tag{7}$$

The reference (α, β) provides the stator flux components as in (8) and (9).

$$\psi_{s\alpha} = \int_0^t (V_{s\alpha} - R_s I_{s\alpha}) dt \tag{8}$$

$$\psi_{s\beta} = \int_0^t (V_{s\beta} - R_s I_{s\beta}) dt \tag{9}$$

The creation of inputs for hysteresis comparators and their related reference values, $\psi_{s,ref}$, is made possible by the evaluation of the predicted stator $\psi_{s,est}$ and projected electromagnetic torque T_{em}. The inputs from these comparators, which include things like the flux sector number of the hysteresis comparator and its outcomes, are vital for the control table as shown in Table 1. Utilizing this information, the control table selects the appropriate voltage vector (μ_0 to μ_7) for subsequent processing, ensuring effective control and regulation of the system.

Table 1. Switching table

e_ψ	e_{Te}	S(1)	S(2)	S(3)	S(4)	S(5)	S(6)
1	1	μ_2 [110]	μ_3 [010]	μ_4 [011]	μ_5 [001]	μ_6 [101]	μ_1 [100]
1	0	μ_7 [111]	μ_0 [000]	μ_7 [111]	μ_0 [000]	μ_7 [111]	μ_0 [000]
1	-1	μ_6 [101]	μ_1 [100]	μ_2 [110]	μ_3 [010]	μ_4 [011]	μ_5 [001]
-1	1	μ_3 [010]	μ_4 [011]	μ_5 [001]	μ_6 [101]	μ_1 [100]	μ_2 [110]
-1	0	μ_0 [000]	μ_7 [111]	μ_0 [000]	μ_7 [111]	μ_0 [000]	μ_7 [111]
-1	-1	μ_5 [001]	μ_6 [101]	μ_1 [100]	μ_2 [110]	μ_3 [010]	μ_4 [011]

3.2. Indirect flux-oriented control

Field-oriented control is a widely adopted approach for variable speed drives of asynchronous machines, known for its ability to provide precise speed and torque control, along with high static and dynamic performance. Similar to a regular motor, it provides a great transient response and permits

independent control of the electromagnetic flux and torque. A coordinate system (d-q) that is aligned with the rotating ψ_{dr} is used to implement the control in FOC. The quadrature component ψ_{qr} is deleted while the flux's direct component is preserved since the d-axis corresponds with the rotor ψ_r. This decoupling between the excitation current controlling the armature current linked to the torque and the flux allows for effective control of both quantities, resembling the characteristics observed in DC motors [20], [21]. The following orientation condition expresses this:

$$\psi_{qr} = 0 \; ; \psi_{dr} = \psi_r = M.I_{sd} \tag{10}$$

An expression for electromagnetic torque is:

$$T_{em} = \frac{3}{2}\frac{M}{L_r}P\psi_r I_{sq} \tag{11}$$

Analyzing the equations in the following system will yield the control formulas as in (12) and (13).

$$I_{sd\_ref} = \frac{1}{M}\psi_{r\_ref} \tag{12}$$

$$I_{sq\_ref} = \frac{2}{3}\frac{L_r}{PM}\frac{T_{em}}{\psi_{r\_ref}} \tag{13}$$

The proposed indirect flux-oriented control (IFOC) technique employed in this study eliminates the need for rotor flux magnitude estimation. Instead, a flux-weakening block is utilized to control the flux in an open loop fashion, where a reference value is set. The position of the stator frequency w_s is determined by integrating the calculated speed and slip frequency. This approach simplifies the control strategy by removing the requirement for direct measurement or estimation of the rotor flux magnitude, enhancing the overall efficiency and robustness of the control system.

$$\theta_s = \int w_s.\,dt = \int \left(w_r + \frac{M}{T_r}\frac{I_{sq\_ref}}{\psi_{r\_ref}}\right)dt \tag{14}$$

In order to achieve speed regulation, a PI-type controller is implemented to minimize the deviation between the desired speed and the estimated speed. Furthermore, to control the direct and quadrature stator currents, two PI controllers are used. To address the interactions between the two orthogonal axes, a decoupling block is introduced, ensuring proper decoupling and control of the d and q axes. This approach allows for precise control of the stator currents, leading to improved performance and efficiency of the system. The current controllers extract the voltage references necessary to achieve the desired flux and electromagnetic torque through an inverse park transformation. Subsequently, the voltage waveforms required are generated, and the sine-triangle PWM technique is employed to drive the voltage inverter. Figure 2 illustrates a diagram of the comprehensive system model, incorporating the developed controller for the induction motor controlled by IFOC.
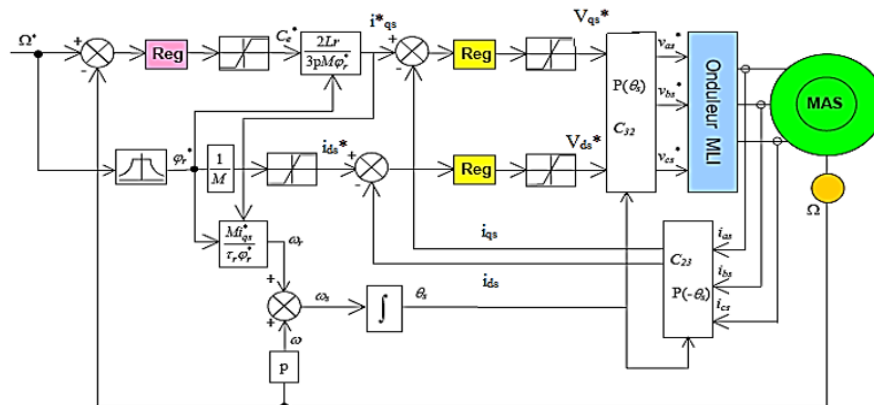

Figure 2. The vector control diagram for an induction motor

3.3. Fuzzy logic-based torque control

In the context of controlling an asynchronous motor driven by a two-level voltage inverter, Figure 3 shows a DTC fuzzy logic control approach. To determine electromagnetic torque and the stator flux at each sampling interval, the measured stator current and applied voltage vectors (15) to (17) are utilized. However, the accuracy of the response is not always guaranteed, especially when dealing with minor faults and when the same switch state used for normal operation is applied to handle severe issues. To enhance system performance, the voltage vector can be calculated based on the torque mistake and flux error data. A fuzzy logic controller, as opposed to a hysteresis comparator and a typical switching table, is used to accomplish this. The three inputs for the proposed fuzzy logic controller (FLC) are the stator flux mistake, the angle indicating the location of the flux, and the torque error. S_a, S_b, and S_c are three other outputs that it has in order to boost system performance. Figure 4 depicts a block diagram of how fuzzy logic works. It is composed of three major components: fuzzification, inference, and defuzzification [22].

$$\Delta T_e = T_{e\_ref} - T_e \tag{15}$$

$$\Delta \psi_s = \psi_{s\_re} - \psi_s \tag{16}$$

$$\theta_s = arctan\left(\frac{\psi_{s\beta}}{\psi_{s\alpha}}\right) \tag{17}$$
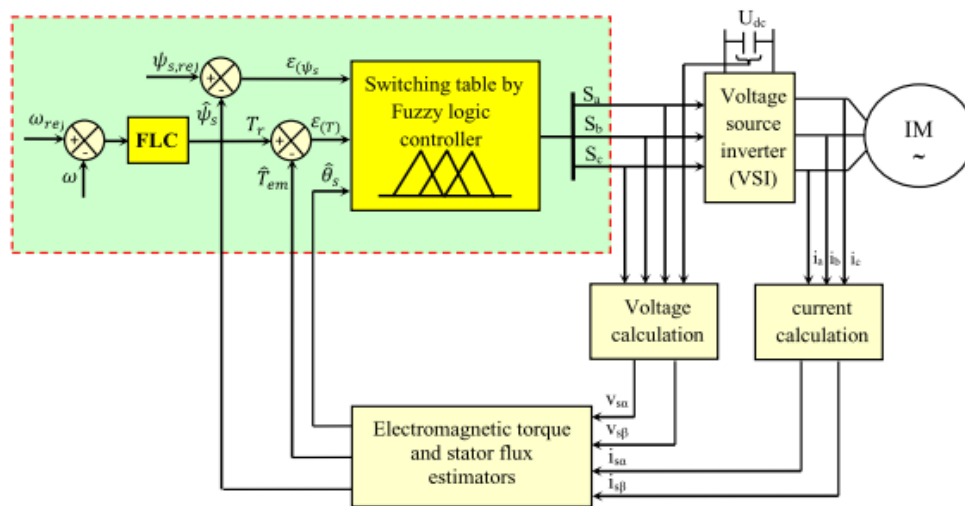
Figure 3. Diagram of DTC-fuzzy control for induction machine: a synoptic overview
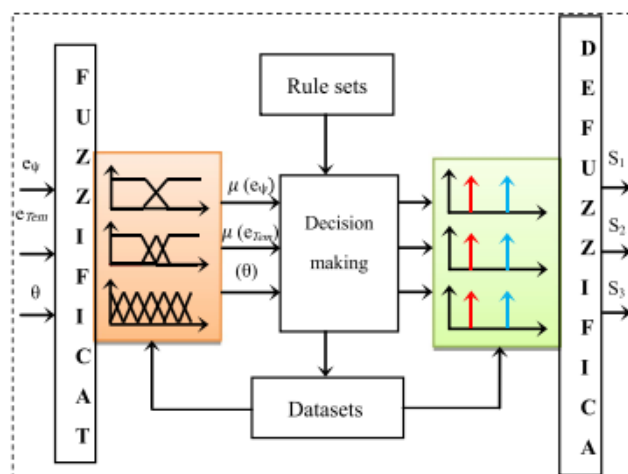
Figure 4. Schematic of a fuzzy controller

3.3.1. Fuzzification

The FLC takes physical input variables and fuzzifies them by converting them into linguistic variables, which involves specifying membership functions for each input variable as depicted in Figure 5. For the first input variable, flux error, N and P, two linguistic variables are assigned to represent positive and negative flux errors. Figure 5(a) displays the trapezoidal membership functions selected for the two fuzzy sets (P and N). The electromagnetic torque error is the next input parameter, N stands for null torque error, P for positive torque mistake, and Z for positive torque error as shown in Figure 5(b). The membership functions for the sets are represented using trapezoidal and triangular functions in Figure 4. The third input variable is the location of the flux in the stator vector, and it is separated into six fuzzy sets (θ_1 to θ_6), each with a triangular membership function is shown in Figure 5(c). the output variable representing inverter switching state is divided into three output groups (S_a, S_b, and S_c), with each group's discourse universe being divided into two fuzzy sets (0 and 1) using a singleton form membership function [23], [24].
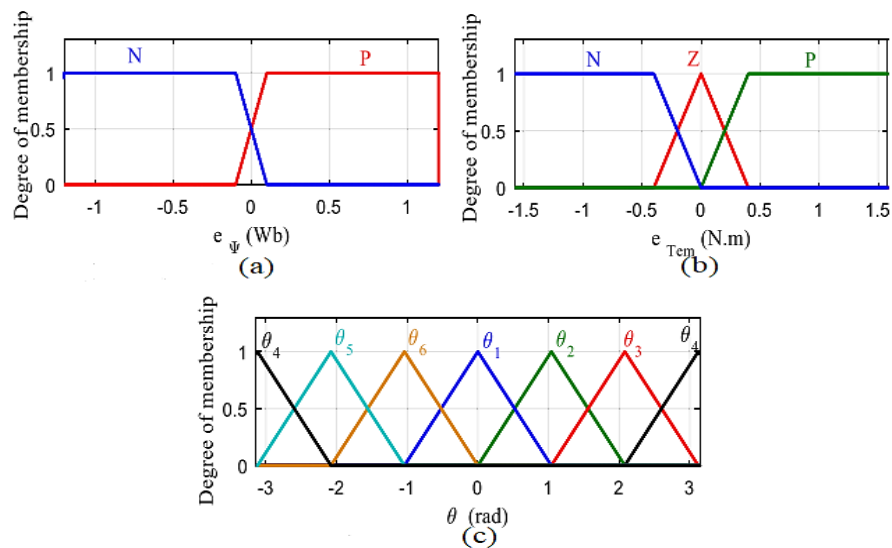

Figure 5. Membership function inputs:(a) Stator flux error, (b) Torque error, and (c) Flux position

3.3.2. Fuzzification block

In the suggested control scheme for induction machine systems, the FLC block is a key component. This block is responsible for handling input variables, converting them into appropriate linguistic values, and providing output variables that represent the inverter switching states. To make sure the control procedure is accurate, the FLC block first establishes the value ranges for the input variables' membership functions. Triangular and trapezoidal sets are used to represent membership functions, and fuzzy sets Z, N, and P are employed to explain T_{em} error and the ψ_s fault. Moreover, to succeed precise control over the stator flux angle sector, the FLC block divides it into six sets of fuzzy values denoted as θ_1 to θ_2. Moreover, to achieve precise control over the stator flux angle sector, the FLC block divides it into six sets of fuzzy values denoted as θ_1 to θ_2. These fuzzy sets reflect the stator flux distribution over six sectors in the (α, β) standard frame, enabling precise flux control. Finally, the output variable, which represents the inverter switching states, is divided into three output singletons (S_1, S_2, and S_3) based on two fuzzy sets, zero and one. This categorization ensures effective control over the inverter switching operations, resulting in superior dynamic performance and reduced torque and flux ripples. In Table 2, we group together 36 fuzzy rules that are determined by using membership functions of input variables to select the appropriate switching state [25], [26].

Table 2. Switching fuzzy rules

e_ψ	e_{Te}	θ_1	θ_2	θ_3	θ_4	θ_5	θ_6
P	P	110	010	011	001	101	100
P	Z	111	000	111	000	111	000
P	N	101	100	110	010	011	001
N	P	010	011	001	101	100	110
N	Z	000	111	000	111	000	111
N	N	001	101	100	110	010	011

3.3.3. Foundations of control rules and inference mechanisms

The fuzzy controller employs linguistic variables to draw inferences based on a set of rules. The rule base encapsulates the operator's knowledge in controlling the process. By utilizing linguistic rules, a fuzzy rule system enables the description of a transfer function between input and output variables. In this particular case, the fuzzy control system comprises 36 rules, outlined in Table 1. The inference method employed is the Mamdani method, which utilizes the Max-Min approach for decision-making. The system's most important block also specifies the value ranges for the functions that determine the membership of the output variables. After that, this block fuzzifies the inferred fuzzy signal in order to provide a non-fuzzy control signal. The most well-known and often employed techniques for this procedure entail figuring out the center of gravity and maximum values. The latter technique was used in this investigation. Figure 6 displays membership formulas for voltage vector membership functions in the output space.
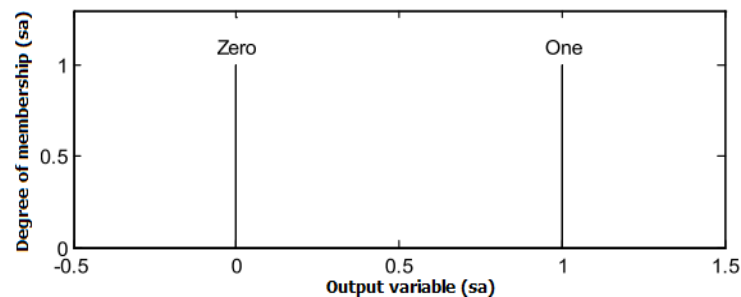

Figure 6. Output membership functions

4.   RESULTS AND DISCUSSION

Figures 7 to 18 illustrate the simulation outcomes for the suggested control techniques, which include indirect field-oriented control, DTC utilizing hysteresis controllers, and fuzzy logic-based DTC of an IM powered by inverter. The speed is fixed at 156 rad/s, with a load torque of 0 Nm from 0 to 0.2 seconds, 10 Nm from 0.2 to 0.7 seconds, and 5 Nm from 0.7 to 1 second. This study compares the effectiveness of these control methods for an induction machine, considering stator flux, stator current, speed, response time, and electromagnetic torque as the evaluation criteria. With regards to speed, indirect field-oriented control, as shown in Figure 7, generally exhibits longer response times due to its reliance on flux and torque regulators. Traditional direct control, as shown in Figure 8, demonstrates shorter response times as it allows for more direct control of motor speed.
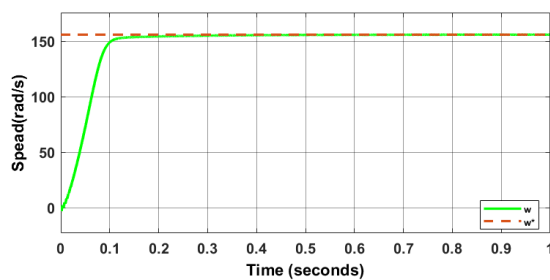

Figure 7. Rotation speed using IFOC
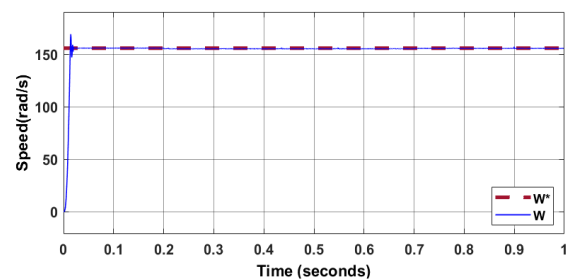
Figure 8. Rotation speed using DTC

Fuzzy logic direct control, as shown in Figure 9, also offers fast response times by adjusting control parameters in real-time based on operating conditions. Regarding electromagnetic torque, indirect field-oriented control, as shown in Figure 10, achieves relatively high precision but may result in undesired torque fluctuations. Traditional direct control, as shown in Figure 11, typically provides a more stable torque output, while fuzzy logic direct control, as shown in Figure 12, can effectively suppress torque fluctuations by adapting control parameters to the operating conditions. In terms of stator flux, indirect field-oriented control, as shown in Figure 13, is designed to maintain a constant stator flux, ensuring proper motor operation. Traditional direct control and fuzzy logic direct control, as shown in Figures 14 and 15, also maintain a stable

stator flux, albeit with some variations due to control parameter adjustments. For stator currents, all control techniques, as shown in Figures 16, 17, and 18, effectively regulate the currents to meet operational requirements. However, fuzzy logic direct control demonstrates better suppression of current harmonics by dynamically adjusting control parameters to minimize disturbances. During startup, indirect field-oriented control offers a smooth startup, enabling precise control of the flux and torque right from the initial moments. Nevertheless, it might exhibit longer response times and necessitate a more intricate implementation. On the other hand, traditional direct control is straightforward and responsive during startup, enabling direct control of the speed and torque. However, it might be susceptible to fluctuations and instabilities during startup, potentially requiring supplementary mechanisms. Fuzzy logic direct control adjusts in real-time to operating conditions, including startup, to ensure a seamless startup process. Nonetheless, its implementation necessitates accurate system modeling and additional expertise. In terms of the overall comparison of the three control techniques for an induction machine, fuzzy logic direct control stands out for its fast response times, ability to suppress torque fluctuations, and adaptability to varying operating conditions. However, each control technique has its own strengths and limitations, and the most appropriate strategy is determined by the particular application requirements and performance goals.
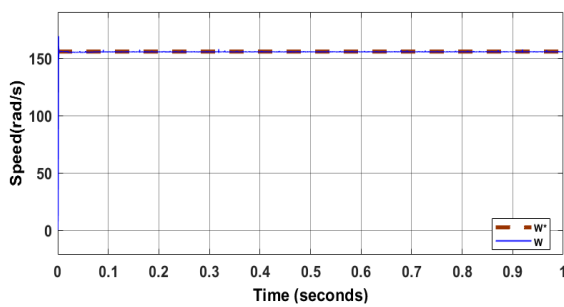
Figure 9. Rotation speed using fuzzy logic
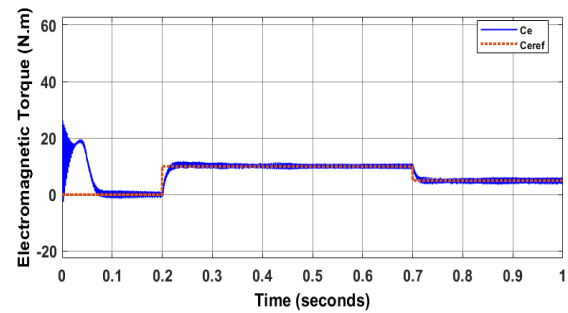
Figure 10. Magnetic torque using IFOC
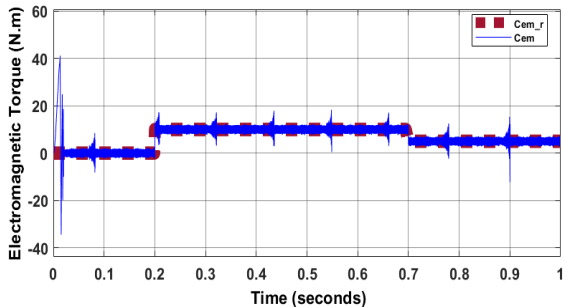
Figure 11. Magnetic torque using DTC
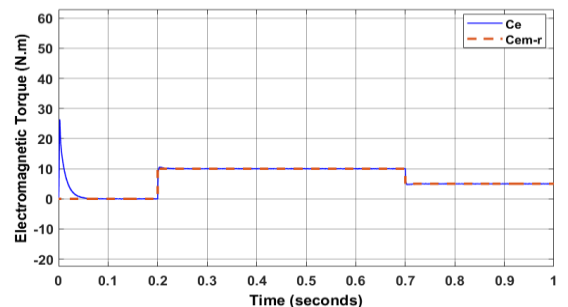
Figure 12. Magnetic torque using fuzzy logic
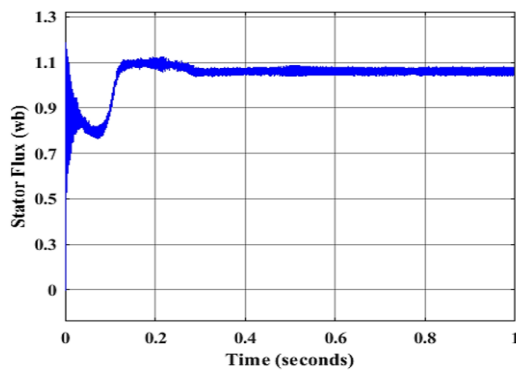
Figure 13. Stator flux using IFOC
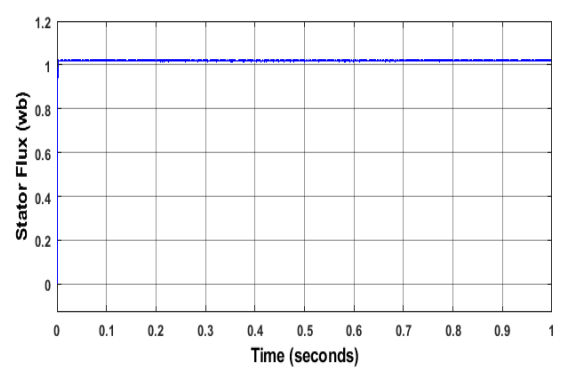
Figure 14. Stator flux using DTC
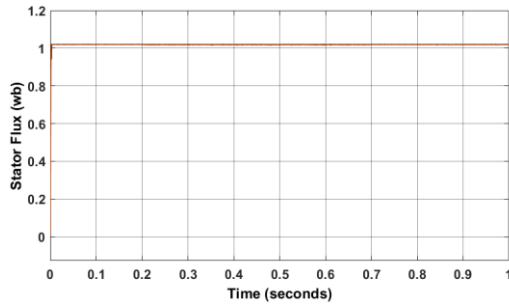
Figure 15. Stator flux using fuzzy logic
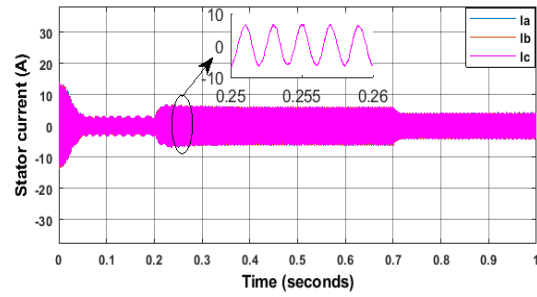
Figure 16. Stator current using indirect IFOC
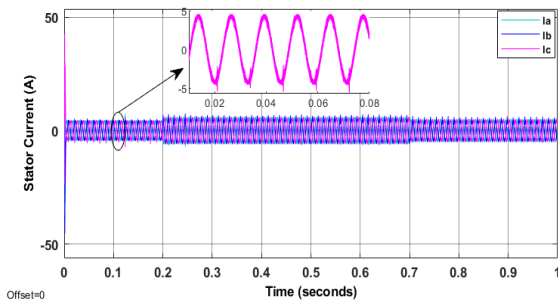

Figure 17. Stator current using DTC
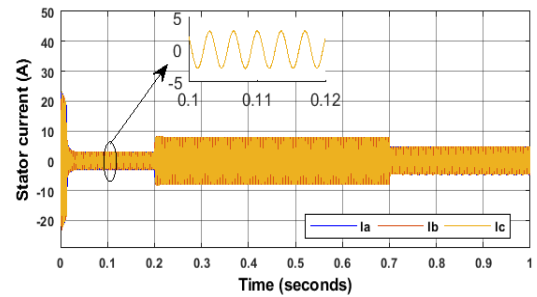
Figure 18. Stator current using fuzzy logic

4.1. Comparative analysis

Table 3 presents a comparative analysis of the performance of three control methods: indirect flux-oriented controllers (IFOC), traditional DTC, and fuzzy logic-based DTC. The evaluation is conducted under both transient and steady-state circumstances, considering key parameters such as rise time, overshoot, and settling time. The results presented in the table highlight the superior performance of fuzzy logic-based DTC. Compared to IFOC and traditional DTC controllers, the fuzzy logic-based DTC demonstrates faster rise time, shorter settling time, and reduced overshoot. This signifies that the fuzzy logic-based approach surpasses both IFOC and traditional DTC controllers, showcasing the induction motor's remarkable ability to achieve precise and rapid speed adjustments without experiencing overshoot or inaccuracies in steady-state operation. To further support these findings, the evolution of the stator current is depicted in Figures 16, 17, and 18. Notably, the motor utilizing the fuzzy logic-based DTC exhibits an excellent sinusoidal waveform in the stator current, indicative of well-controlled performance. Conversely, the stator currents in IFOC and traditional DTC controllers exhibit significant harmonics, suggesting less optimal control. These results underscore the effectiveness of fuzzy logic-based DTC in achieving superior performance and control precision for induction motors. The ability to mitigate harmonics and maintain a desirable sinusoidal waveform in the stator current reinforces the advantages of the fuzzy logic-based approach.

Table 3. Comparative study between proposed strategies

Control strategies	Settling time (sec)	%Overshoot	Rise time (sec)
DTC	0.0295	0.5034	0.0193
DTC based on fuzzy logic	0.01276	0.4173	0.0102
IFOC	0.07312	1.9471	0.0523

5.   CONCLUSION

This article presents a novel enhancement to the DTC algorithm for IM by utilizing intelligent approaches based on fuzzy logic. The proposed method involves replacing the switching selector block and the two hysteresis controllers with a fuzzy logic controller. Through extensive simulations, it is demonstrated that the proposed strategy outperforms conventional DTC and field-oriented control techniques. Comparative analysis between fuzzy logic-based control and other established methods, such as flux-oriented control or conventional DTC, reveals similar results, further validating the efficiency of fuzzy logic-based enhancements in the DTC strategy. The fuzzy logic-based algorithm exhibits faster dynamic responses in the

transient state and significantly reduces torque ripples in the steady state, regardless of load or no-load conditions. The key improvements observed in the fuzzy logic-based approach encompass a reduction in response time, speed rejection time, and flux and torque oscillations, along with a notable reduction in total harmonic distortion (THD) in the stator current. To advance this research, future work will focus on implementing the fuzzy logic-based DTC using a field programmable gate arrays-based (FPGA) test platform within our laboratory.

REFERENCES

[1] E. Robles, M. Fernandez, J. Andreu, E. Ibarra, J. Zaragoza, and U. Ugalde, "Common-mode voltage mitigation in multiphase electric motor drive systems," *Renewable and Sustainable Energy Reviews*, vol. 157, Apr. 2022, doi: 10.1016/j.rser.2021.111971.

[2] B. A. Alsati, G. I. Ibrahim, and R. R. Moussa, "Study the impact of transient state on the doubly fed induction generator for various wind speeds," *Journal of Engineering and Applied Science*, vol. 70, no. 1, Dec. 2023, doi: 10.1186/s44147-023-00232-6.

[3] P. Q. Khanh and H. P. H. Anh, "Advanced PMSM speed control using fuzzy PI method for hybrid power control technique," *Ain Shams Engineering Journal*, Mar. 2023, doi: 10.1016/j.asej.2023.102222.

[4] H. Albalawi, S. A. Zaid, M. E. El-Shimy, and A. M. Kassem, "Ant colony optimized controller for fast direct torque control of induction motor," *Sustainability*, vol. 15, no. 4, Feb. 2023, doi: 10.3390/su15043740.

[5] Y.-F. Jia *et al.*, "Control strategy for an open-end winding induction motor drive system for dual-power electric vehicles," *IEEE Access*, vol. 8, pp. 8844–8860, 2020, doi: 10.1109/ACCESS.2020.2964105.

[6] H. Salime, B. Bossoufi, Y. El Mourabit, and S. Motahhir, "Robust nonlinear adaptive control for power quality enhancement of PMSG wind turbine: experimental control validation," *Sustainability*, vol. 15, no. 2, Jan. 2023, doi: 10.3390/su15020939.

[7] S. Palackappillil and A. E. Daniel, "Switching function parameter variation analysis of a quasi-sliding mode controlled induction motor drive," *International Journal of Power Electronics and Drive Systems (IJPEDS)*, vol. 13, no. 2, pp. 733–743, Jun. 2022, doi: 10.11591/ijpeds.v13.i2.pp733-743.

[8] R. K. Bindal and I. Kaur, "Torque ripple reduction of induction motor using dynamic fuzzy prediction direct torque control," *ISA Transactions*, vol. 99, pp. 322–338, Apr. 2020, doi: 10.1016/j.isatra.2019.09.012.

[9] R. Senthil Kumar *et al.*, "A combined HT and ANN based early broken bar fault diagnosis approach for IFOC fed induction motor drive," *Alexandria Engineering Journal*, vol. 66, pp. 15–30, Mar. 2023, doi: 10.1016/j.aej.2022.12.010.

[10] I. Takahashi and T. Noguchi, "A new quick-response and high-efficiency control strategy of an induction motor," *IEEE Transactions on Industry Applications*, vol. IA-22, no. 5, pp. 820–827, Sep. 1986, doi: 10.1109/TIA.1986.4504799.

[11] D. Murillo-Yarce, B. Araya, C. Restrepo, M. Rivera, and P. Wheeler, "Impact of sequential model predictive control on induction motor performance: comparison of converter topologies," *Mathematics*, vol. 11, no. 4, Feb. 2023, doi: 10.3390/math11040972.

[12] P. Gangsar and R. Tiwari, "Signal based condition monitoring techniques for fault detection and diagnosis of induction motors: a state-of-the-art review," *Mechanical Systems and Signal Processing*, vol. 144, Oct. 2020, doi: 10.1016/j.ymssp.2020.106908.

[13] Z. Mekrini and S. Bri, "High –performance using neural networks in direct torque control for asynchronous machine," *International Journal of Electrical and Computer Engineering (IJECE)*, vol. 8, no. 2, pp. 1010–1017, Apr. 2018, doi: 10.11591/ijece.v8i2.pp1010-1017.

[14] O. Asvadi-Kermani, B. Felegari, and H. Momeni, "Adaptive constrained generalized predictive controller for the PMSM speed servo system to reduce the effect of different load torques," *e-Prime - Advances in Electrical Engineering, Electronics and Energy*, vol. 2, 2022, doi: 10.1016/j.prime.2022.100032.

[15] F. Wang, H. Xie, Q. Chen, S. A. Davari, J. Rodriguez, and R. Kennel, "Parallel predictive torque control for induction machines without weighting factors," *IEEE Transactions on Power Electronics*, vol. 35, no. 2, pp. 1779–1788, Feb. 2020, doi: 10.1109/TPEL.2019.2922312.

[16] Z. Mekrini and S. Bri, "Performance of an indirect field-oriented control for asynchronous machine," *International Journal of Engineering and Technology*, vol. 8, no. 2, pp. 726–733, 2016.

[17] A. Narendra, V. Naik N, A. K. Panda, and R. K. Lenka, "Solar PV fed FSVSI based variable speed IM drive using ASVM technique," *Engineering Science and Technology, an International Journal*, vol. 40, Apr. 2023, doi: 10.1016/j.jestch.2023.101366.

[18] S. Toledo *et al.*, "Predictive control applied to matrix converters: a systematic literature review," *Energies*, vol. 15, no. 20, Oct. 2022, doi: 10.3390/en15207801.

[19] M. Depenbrock, "Direct self-control (DSC) of inverter-fed induction machine," *IEEE Transactions on Power Electronics*, vol. 3, no. 4, pp. 420–429, Oct. 1988, doi: 10.1109/63.17963.

[20] G. Kamalapur and M. S. Aspalli, "Direct torque control and dynamic performance of induction motor using fractional order fuzzy logic controller," *International Journal of Electrical and Computer Engineering (IJECE)*, vol. 13, no. 4, pp. 3805–3816, Aug. 2023, doi: 10.11591/ijece.v13i4.pp3805-3816.

[21] Y. Baala and S. Bri, "Torque estimator using MPPT method for wind turbines," *International Journal of Electrical and Computer Engineering (IJECE)*, vol. 10, no. 2, pp. 1208–1219, Apr. 2020, doi: 10.11591/ijece.v10i2.pp1208-1219.

[22] Y. Boujoudar *et al.*, "Fuzzy logic-based controller of the bidirectional direct current to direct current converter in microgrid," *International Journal of Electrical and Computer Engineering (IJECE)*, vol. 13, no. 5, pp. 4789–4797, Oct. 2023, doi: 10.11591/ijece.v13i5.pp4789-4797.

[23] V. Pushparajesh, N. B. M., and H. B. Marulasiddappa, "Hybrid intelligent controller based torque ripple minimization in switched reluctance motor drive," *Bulletin of Electrical Engineering and Informatics (BEEI)*, vol. 10, no. 3, pp. 1193–1203, Jun. 2021, doi: 10.11591/eei.v10i3.3039.

[24] Q. Al Azze and I. A.-R. Hameed, "Reducing torque ripple of induction motor control via direct torque control," *International Journal of Electrical and Computer Engineering (IJECE)*, vol. 13, no. 2, pp. 1379-1386, Apr. 2023, doi: 10.11591/ijece.v13i2.pp1379-1386.

[25] M. Aktas, K. Awaili, M. Ehsani, and A. Arisoy, "Direct torque control versus indirect field-oriented control of induction motors for electric vehicle applications," *Engineering Science and Technology, an International Journal*, vol. 23, no. 5, pp. 1134–1143, Oct. 2020, doi: 10.1016/j.jestch.2020.04.002.

[26] G. Rigatos, M. Abbaszadeh, B. Sari, P. Siano, G. Cuccurullo, and F. Zouari, "Nonlinear optimal control for a gas compressor driven by an induction motor," *Results in Control and Optimization*, vol. 11, Jun. 2023, doi: 10.1016/j.rico.2023.100226.

BIOGRAPHIES OF AUTHORS

Radouan Gouaamar obtained his master's degree in renewable energy engineering, specializing in energy efficiency, network, and electrical energy from the multidisciplinary faculty of Beni Mellal in Morocco in 2020. In 2017, he received a bachelor's degree in renewable energy. He is currently a Ph.D. student at Moulay Ismail University in Meknes, Morocco. His research interests lie in the fields of electrical engineering, power engineering, and renewable energies. He can be contacted at r.gouaamar@edu.umi.ac.ma.

Seddik Bri is a full professor in the Electrical Engineering Department, responsible for the Material and Instrumentation Group at the High School of Technology, Moulay Ismail University, Meknes-Morocco. His research interests are in communication systems with 200 published conferences. He can be contacted at email: s.bri@umi.ac.ma or briseddik@gmail.com.

Zineb Mekrini received her Ph.D. degree in electrical engineering from Moulay Ismail University, Meknes, Morocco, in 2018. She is now a professor at the Electrical Engineering Department in the Faculty of Sciences and Techniques of Tangier, Abdelmalek-Essaadi University, Morocco. Her current research includes the control of power converters, renewable energy, and fuzzy logic control. She can be contacted at zineb.mekrini@gmail.com.